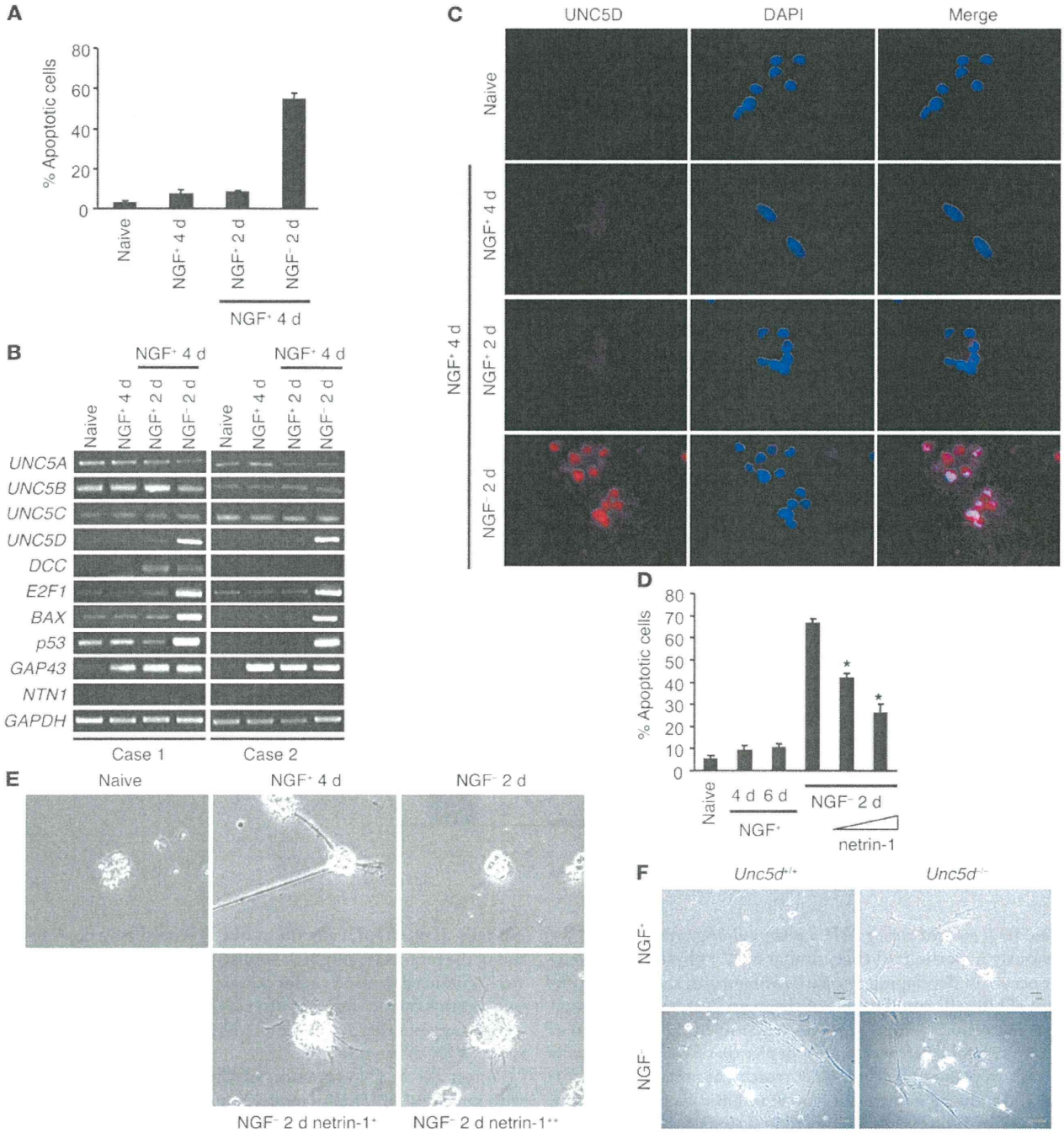

Figure 3

UNC5D is involved in NGF withdrawal–induced apoptosis. (**A**) Apoptosis assay of primary NB cells from a stage 1 tumor treated with NGF for 4 days, followed by NGF treatment or NGF withdrawal for 2 additional days as indicated. Data represent mean ± SD. (**B**) Semiquantitative RT-PCR analysis of primary NB cells from case 1 (9 months old, stage 1, single copy of *MYCN*, high TRKA expression, and aneuploidy) and case 2 (18 months old, stage 3, single copy of *MYCN*, high TRKA expression, and aneuploidy) treated as in **A**. (**C**) Confocal images of UNC5D immunostaining in primary NB cells treated as in **A**. Nuclei were stained with DAPI. Original magnification, ×200. (**D**) Apoptosis assay of primary NB cells treated as in **A**, with or without addition of increasing amounts of netrin-1. Data represent mean ± SD. $^*P < 0.01$. (**E**) Light microscopic images of primary NB cells in **D**. Original magnification, ×40. (**F**) Light microscopic images of primary sympathetic neurons after NGF depletion. Primary sympathetic neurons were isolated from SCG of P0 wild-type and *Unc5d*$^{-/-}$ mice and cultured for 5 days with NGF-containing medium. Neurons were then treated with or without NGF for an additional 3 days. Scale bars: 100 μm.

Table 1
Increased number of DRG (L3–L5) neurons in *Unc5d*$^{-/-}$ mice at P0

Genotype	*n*	No. cells/DRG
Wild-type	13	6,040 ± 242
Unc5d$^{-/-}$	11	7,286 ± 240[A]

Data represent mean ± SEM. [A]P = 0.0015 vs. wild-type.

tem commonly used for studying NGF deprivation–mediated neuronal death. Similar to human primary NB cells, induction of *UNC5D* was also observed in PC12 cells during the early phase of NGF depletion–induced apoptosis (Supplemental Figure 3, A and B). To further elucidate the involvement of UNC5D in NGF withdrawal–triggered apoptosis, we knocked down UNC5D with Accell siRNA in PC12 cells. As a result, UNC5D-knockdown PC12 cells had attenuated cell death in response to NGF deprivation (Supplemental Figure 3F).

Thus, the netrin-1 receptor UNC5D appears to play a critical role in NGF depletion–induced apoptosis, both in human favorable NB cells and in rodent neurons.

UNC5D is cleaved by caspases 2 and 3. Notably, induced UNC5D was detected in the nuclei using the antibody recognizing the C-terminal region of UNC5D (Figure 3C), which indicates that UNC5D may function in the nucleus. Amino acid sequence alignment showed that UNC5D possessed a conserved consensus caspase cleavage sequence, VDVID^{416}, recognized by both caspase 2 and caspase 3/7 (Figure 4A), which suggests that the UNC5D receptor may be cleaved by caspases. We therefore transfected UNC5D into U2OS cells, which underwent apoptotic cell death accompanied by the activation of caspase 3 (Figure 4B). Surprisingly, overexpressed UNC5D protein was detected as several smaller bands besides the full-length one by a specific antibody recognizing the C terminus of UNC5D. Those smaller bands partially disappeared in the presence of a caspase 3/7 inhibitor and completely with the addition of the pan-caspase inhibitor zVAD-fmk (Figure 4C). Furthermore, in vitro caspase cleavage assay revealed that caspases 2 and 3 both cleaved UNC5D at the D416 site, generating a fragment of approximately 60 kDa (Supplemental Figure 4, A and B), which was detectable in UNC5D-expressing cells but not in D416N mutant–expressing cells in response to cisplatin (CDDP; Figure 4D). These data clearly showed that UNC5D was a direct substrate of caspases 2 and 3.

Caspase-released UnICD translocates into the nucleus. To investigate whether UNC5D nuclear staining was due to nuclear translocation of the intracellular fragment of UNC5D (UnICD) released by caspases, we next introduced UnICD into U2OS cells. As expected, expressed UnICD was present predominantly in the nucleus (Figure 4E and Supplemental Figure 4D). Moreover, the nuclear signals were observed in full-length UNC5D–transfected cells, but not in those treated with a pan-caspase inhibitor or transfected with the D416N mutant (Figure 4E). Furthermore, we transfected U2OS cells with the plasmid encoding mouse UNC5D with a FLAG-tag attached to the N terminus of the protein. The amino acid sequence of mouse UNC5D has 96% similarity to the human homolog. Double immunostaining with monoclonal anti-FLAG antibody and polyclonal anti-UNC5D antibody recognizing the C terminus demonstrated that the nuclear signals were detected only by the anti-UNC5D antibody; that is, the C-terminal fragment of UNC5D had entered into the nucleus (Supplemental Figure 4C). Taken together, our results demonstrated that the caspase-released UnICD translocated into the nucleus. Furthermore, nuclear expression of UNC5D was also observed in regressing NB tissue obtained from a patient in stage 1, who had been found by mass screening at the age of 6 months (Figure 4F). However, netrin-1 expression was almost undetectable in the same area.

Previously, we identified that UNC5D is a direct target of p53 (17). In addition to the response to NGF withdrawal, UNC5D was also induced by genotoxic reagents (adriamycin and CDDP) and by TNF-α treatment in p53–wild-type cells (SH-SY5Y and U2OS) and in p53-inactivated HeLa cells (Supplemental Figure 5B), which indicates that *UNC5D* may be inducible in both a p53-dependent and -independent manner in response to multiple stresses. Indeed, besides p53 (17), p63 and p73 also upregulated *UNC5D* mRNA (Supplemental Figure 5C), indicating that *UNC5D* is a common target of the p53 family. Induced UNC5D was cleaved, and then the released UnICD translocated into the nuclei, in U2OS cells as well as the NB cell line SH-SY5Y receiving these cellular stresses (Supplemental Figure 5D). Collectively, these findings suggest that caspase cleavage of UNC5D and subsequent nuclear translocation of UnICD are the common mechanisms that respond to various proapoptotic stimuli.

To further evaluate the functional significance of UNC5D protein cleavage by caspases, we next expressed full-length UNC5D, UnICD, DD, or the D416N mutant in HeLa, U2OS, and HEK293T cells. Introduction of UNC5D, UnICD, and DD into these cells was sufficient to reduce formation of G418-resistant colonies, inhibit anchorage-independent cell growth, and induce apoptosis to similar extents (Figure 5 and Supplemental Figure 4E). However, addition of the pan-caspase inhibitor or expression of the D416N mutant abolished these effects. Thus, the caspase cleavage of UNC5D may be crucial to initiating UNC5D-induced apoptosis, and the C-terminal DD in the released UnICD could be essential to its proapoptotic function.

Coincident with the above observations in human cells, induction of UNC5D and nuclear translocation of the caspase-released UnICD were detected in wild-type mouse embryonic fibroblasts (MEFs) in response to various apoptotic stimuli (Supplemental Figure 6, A–C). Notably, *Unc5d*$^{-/-}$ MEFs showed more substantial resistance to CDDP treatment than the wild-type cells (Supplemental Figure 6D), suggestive of an important role of UNC5D in the regulation of stress-induced apoptosis in mice.

Netrin-1 inhibits the proapoptotic activity of UNC5D by preventing its cleavage. Dependence receptors display 2 completely opposing actions depending on the availability of their ligands (13). We next tested the effect of netrin-1 on the proapoptotic function of UNC5D. Addition of netrin-1 prevented the cleavage of UNC5D as well as that of caspase 3 and PARP in a dose-dependent manner (Figure 6A), inhibited nuclear translocation of UnICD (Figure 6B), and, consequently, suppressed cell death in U2OS cells transfected with full-length UNC5D (Figure 6, C and D), whereas it had no effect in UnICD-expressing cells (Figure 6, B–E). Thus, netrin-1 may inhibit the proapoptotic activity of UNC5D by preventing UNC5D cleavage and subsequent nuclear translocation of released UnICD.

UnICD functions as a transcriptional coactivator. Translocation of UnICD from the cytoplasm into the nucleus implicated the possibility that nuclear UnICD may ultimately promote apoptosis through activation of a set of apoptosis-related genes like NICD

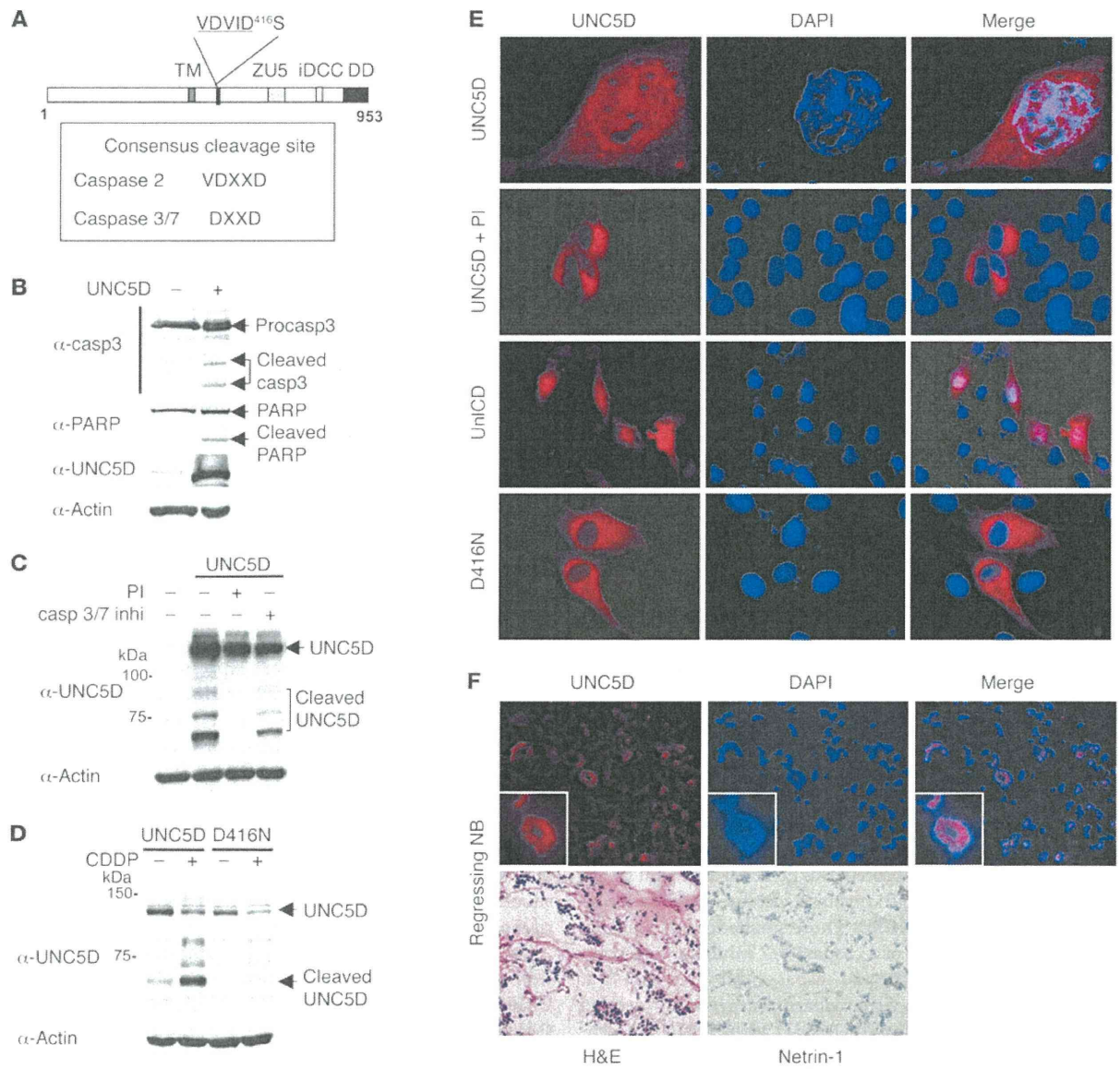

Figure 4

Induced UNC5D is cleaved by caspases, and the released UnICD enters into the nucleus. (**A**) Schematic of UNC5D protein. TM, transmembrane; iDCC, interaction with DCC. (**B**) IB analysis of U2OS cells transfected with UNC5D. (**C**) Overexpressed UNC5D was cleaved by caspases in U2OS cells. UNC5D was probed by a specific antibody recognizing the C terminus. PI, pan-caspase inhibitor; casp3/7 inhi, caspase 3/7 inhibitor. (**D**) IB analysis of U2OS cells transfected with UNC5D or the D416N mutant in response to CDDP. (**E**) Immunofluorescent analysis of U2OS cells transfected with the indicated plasmids. Original magnification, ×400. (**F**) Representative confocal images of UNC5D immunostaining in regressing NB tissue from a stage 1 tumor. Histology of the samples was indicated by H&E staining. Netrin-1 was detected by immunohistochemical staining. Original magnification, ×200; ×400 (insets).

and AICD, intracellular fragments derived from Notch 1 (29) and β-APP (30), respectively. Similar to NICD and AICD, UnICD does not contain the DNA-binding domain, which suggests that UnICD is very likely to act as a coactivator of some transcription factors.

To prove this hypothesis, the Gal4 DNA binding domain–fused UnICD (referred to herein as Gal4-UnICD) was transfected into U2OS or HeLa cells together with pGL4.31, which encodes for the luciferase reporter under the control of the Gal4 upstream activation sequence. As a result, Gal4-UnICD significantly enhanced transcription of the reporter gene in both cell lines (Figure 7A), thereby demonstrating that UnICD has transactivation activity independent of p53. Moreover, the transcriptional activity of UnICD relied on the DD in the C terminus (amino acids 859–953; Figure 7C).

UnICD interacts with E2F1 and selectively transactivates its proapoptotic genes. As reported previously (8, 9) and as shown in Figure 3B, NGF depletion induced expression of *E2F1* in neuronal cells, which suggests that nuclear UnICD may function as a coactivator of E2F1. To explore this possibility, we tested the expression patterns of both

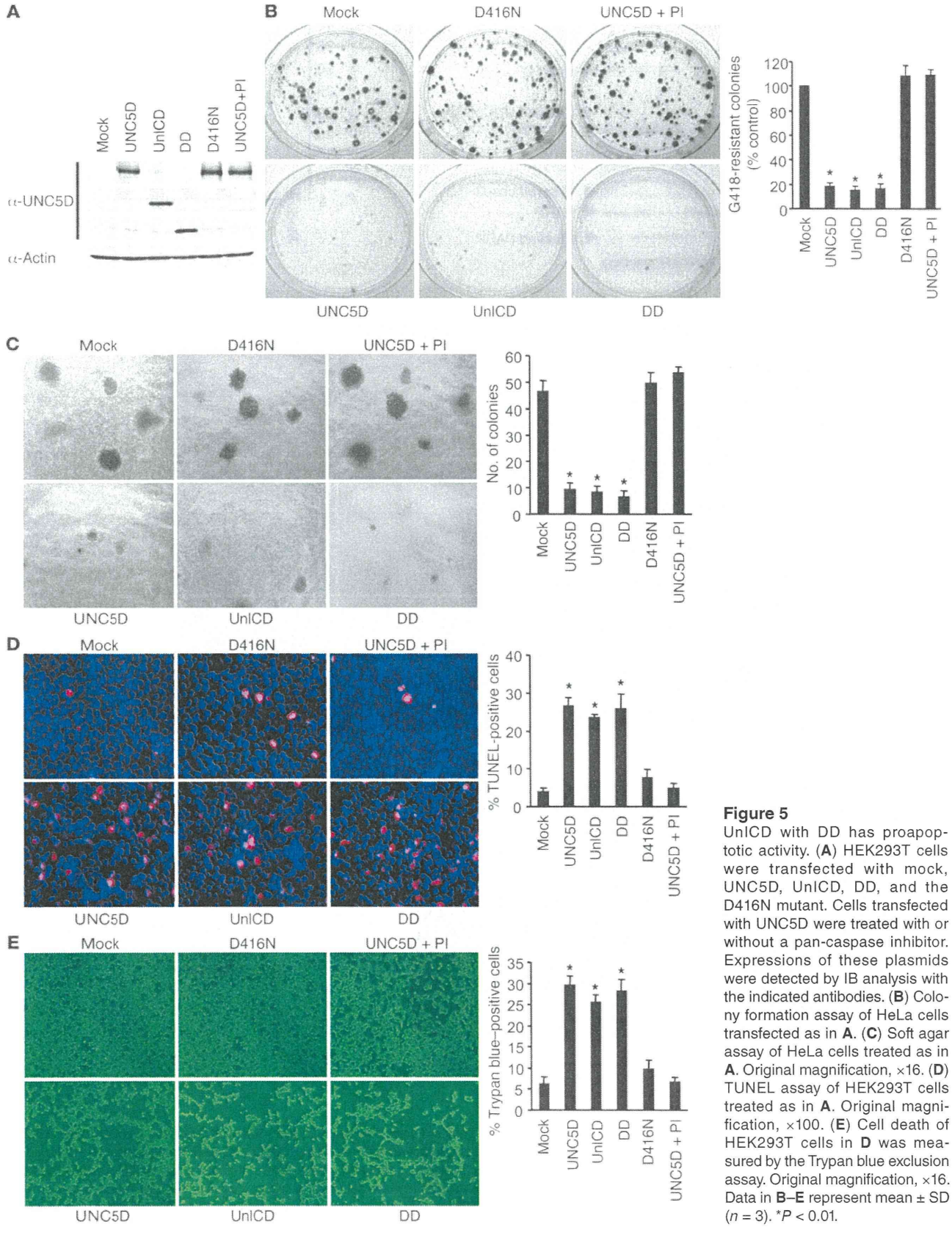

Figure 5
UnICD with DD has proapoptotic activity. (**A**) HEK293T cells were transfected with mock, UNC5D, UnICD, DD, and the D416N mutant. Cells transfected with UNC5D were treated with or without a pan-caspase inhibitor. Expressions of these plasmids were detected by IB analysis with the indicated antibodies. (**B**) Colony formation assay of HeLa cells transfected as in **A**. (**C**) Soft agar assay of HeLa cells treated as in **A**. Original magnification, ×16. (**D**) TUNEL assay of HEK293T cells treated as in **A**. Original magnification, ×100. (**E**) Cell death of HEK293T cells in **D** was measured by the Trypan blue exclusion assay. Original magnification, ×16. Data in **B**–**E** represent mean ± SD ($n = 3$). *$P < 0.01$.

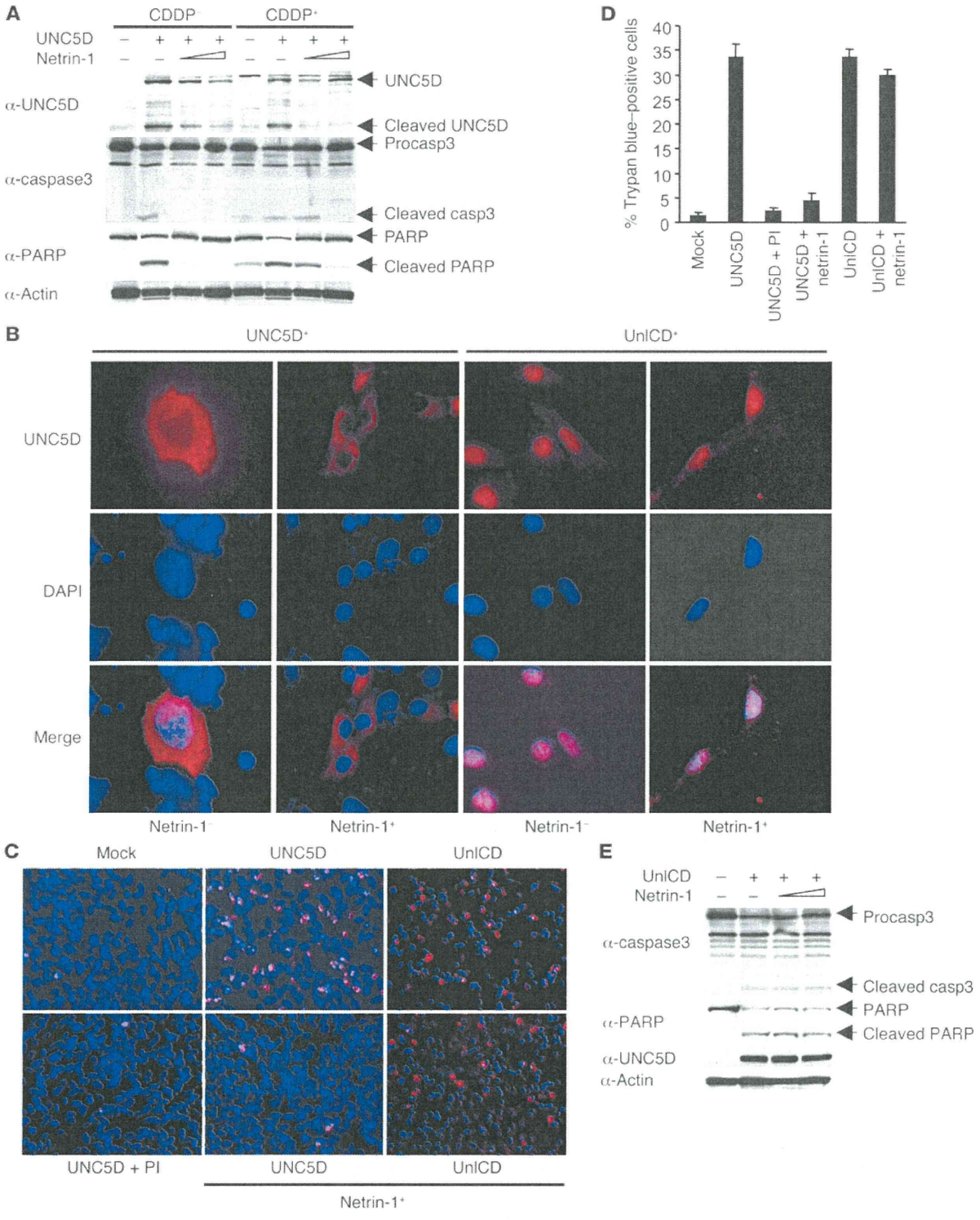

Figure 6

Netrin-1 blocks UNC5D cleavage and UNC5D-induced apoptosis. (**A**) U2OS cells transfected with the indicated plasmids were treated with or without CDDP (40 μM) along with increasing amounts of netrin-1 for 24 hours, followed by IB analysis. (**B**) U2OS cells transfected with UNC5D or UnICD for 24 hours were treated with or without netrin-1 for an additional 24 hours, followed by immunofluorescent staining. Original magnification, ×400. (**C** and **D**) SH-SY5Y cells were transfected with the indicated plasmids and treated with or without a pan-caspase inhibitor or netrin-1. Cell death was evaluated by TUNEL assay (**C**; original magnification, ×100) and Trypan blue exclusion assay (**D**). Data represent mean ± SD (n = 3). (**E**) U2OS cells transfected with UnICD were treated with or without increasing amounts of netrin-1 for 24 hours, followed by IB analysis.

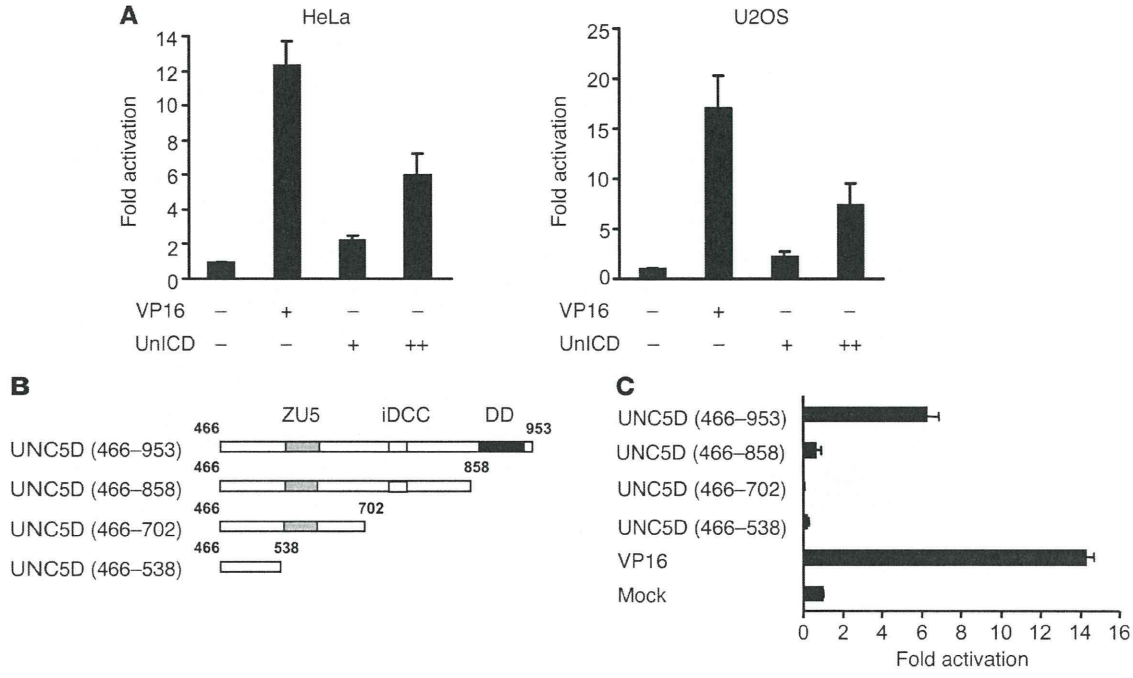

Figure 7

UnICD has transactivation activity. (**A**) Luciferase reporter assay using HeLa and U2OS cells transfected with Gal4-UnICD as indicated. pM-VP16 was used as a positive control. Data represent mean ± SD. (**B**) UnICD and its deletion mutants. (**C**) Luciferase reporter assay using HeLa cells transfected with Gal4-UnICD or its deletion mutants as in **B**. pM-VP16 was used as a positive control. Data represent mean ± SD.

E2F1 and UnICD. As expected, E2F1 was colocalized in the nucleus with UnICD in cotransfected HeLa cells (Supplemental Figure 7C). Moreover, nuclear colocalization of induced UNC5D and E2F1 was observed in both NGF-depleted primary NB cells (Figure 8A) and CDDP-treated HeLa cells (Supplemental Figure 7D). Because of the limited availability of primary NB cells, we investigated the time course of nuclear accumulation of E2F1 and UnICD in response to CDDP in HeLa cells. E2F1 increased in the nucleus at 6 hours after CDDP treatment, followed by UnICD at 12 hours (Figure 8B). Furthermore, coprecipitation of UnICD with E2F1 protein was found in nuclear extracts prepared from not only UnICD/E2F1-cotransfected HeLa cells (Supplemental Figure 7E), but also CDDP-treated SH-SY5Y cells (Figure 8C), indicative of a physical interaction between the 2 molecules in the nucleus.

We next used ChIP assay to examine whether the UnICD/E2F1 complex binds to the promoter of the caspase 7 (*CASP7*) gene, which is a direct target of E2F1 (31). Endogenous UnICD was recruited to the E2F1-binding region in the *CASP7* promoter in response to CDDP (Supplemental Figure 7F), which suggests that UnICD may be involved in the function of E2F1 to induce the target genes.

Because E2F1 possesses the dual function of both oncogene and tumor suppressor (32), we next examined target genes of the UnICD/E2F1 transcriptional complex. Enforced expression of UnICD in SH-SY5Y, U2OS, and HeLa cells induced the expression of E2F1 proapoptotic target genes, including *CASP3*, *CASP7*, *CASP9*, *BID*, and *E2F1* itself (ref. 33, Figure 8D, and Supplemental Figure 7G), which were consistently abrogated by 2 kinds of siRNA against E2F1 in UnICD-transfected HeLa cells (Figure 8E and Supplemental Figure 7B). Similarly, induction of these genes was decreased in *Unc5d*$^{-/-}$ versus wild-type MEFs treated with CDDP (Figure 8F). On the other hand, several growth-promoting target genes of E2F1, including *cyclin E*, *c-Myc*, and *TK1*, were not induced in those UnICD-transfected cells (Supplemental Figure 7H), which suggests that UnICD-mediated apoptosis may be attributed to the selective upregulation of proapoptotic target genes of E2F1. Notably, upregulation of these E2F1 proapoptotic target genes was also observed in NGF-deprived primary NB cells (Supplemental Figure 7I), demonstrating that the UnICD/E2F1 complex plays a pivotal role in NGF depletion–induced apoptosis.

Discussion

The data presented herein revealed that UNC5D is involved in NGF deficiency–induced PCD in human NB cells with NGF dependence. Among UNC5 family members, only UNC5D was strongly induced in response to NGF depletion. High levels of *UNC5D* mRNA expression were significantly associated with favorable outcomes in patients with NB, which has the ability to undergo spontaneous regression. We propose a model whereby NGF deficiency triggers induction of *UNC5D*, *E2F1*, and *p53* in NB cells. Under the relative deficiency of netrin-1, the induced UNC5D is prone to be cleaved by activated caspases, and the released UnICD translocates into the nucleus and forms a complex with E2F1, which in turn selectively induces E2F1 proapoptotic target genes to enhance cell death (Figure 9). *UNC5D* is a direct target of p53 (17); thus, in cooperation with E2F1 and p53, UNC5D may contribute to PCD by intensifying cell death signaling in regressing NBs.

Induction of cell death by each UNC5 family member appears to occur by different mechanisms. UNC5A mediates apoptotic cell death by interacting with NRAGE via its ZU5 domain (34), while UNC5B requires its DD to recruit death-associated protein

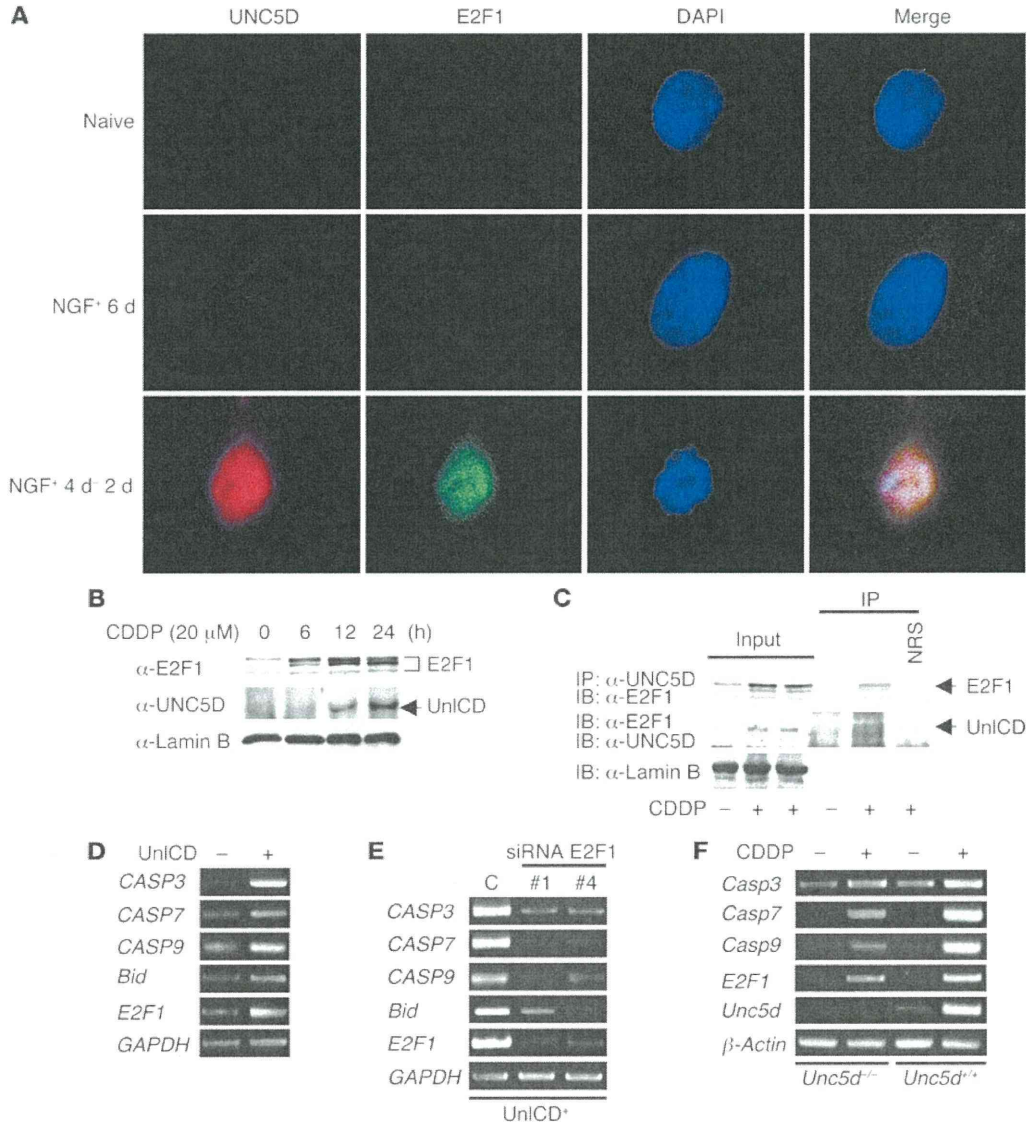

Figure 8

Nuclear UnICD promotes apoptosis as a cofactor of E2F1. (**A**) Immunofluorescent staining of endogenous UNC5D and E2F1 was conducted in primary NB cells treated as in Figure 3A. Original magnification, ×400. (**B**) Nuclear extracts were prepared from HeLa cells treated with CDDP (20 μM) for the indicated time periods and analyzed by IB. (**C**) Nuclear extracts were prepared from SH-SY5Y cells treated with CDDP (10 μM, 24 hours) and subjected to IP, followed by IB with the indicated antibodies. (**D**) Semiquantitative RT-PCR using the cDNAs generated from SH-SY5Y cells transfected with the indicated expression vectors. (**E**) HeLa cells transfected with siRNAs against E2F1 or a negative control for 24 hours were then transfected with UnICD for an additional 48 hours, followed by semiquantitative RT-PCR. (**F**) Expression of the E2F1 proapoptotic targets was measured by semiquantitative RT-PCR in wild-type and *Unc5d*$^{-/-}$ MEFs treated with or without CDDP.

kinase (DAPK) in the induction of apoptosis (35). Intriguingly, only *UNC5D* among the *UNC5* family members was inducible in response to NGF depletion (Figure 3B). In support of this, expression levels of *UNC5D* mRNA were significantly higher in favorable NBs (Figure 1A). High levels of *UNC5D* mRNA expression were significantly associated with favorable outcome in NBs (Figure 1C). In our study, we did not detect a significant increase in the expression levels of *UNC5D* mRNA in stage 4s tumors. One of the reasons may be the small sample number; only 6 of 108 primary NB cases tested in our analysis were stage 4s. In addition, we found that UNC5D was induced only in NGF-deprived NB cells, not in NGF-differentiated ones (Figure 3B). Furthermore, many or most of the NB cells with induced expression of *UNC5D* mRNA might already have died of NGF deficiency in stage 4s tumors. Therefore, it seems that increased expression of *UNC5D* mRNA may not be observed in spontaneously regressing stage 4s tumors in which extensive tumor cell death and differentiation have occurred. To clarify this, a large sample size will need to be investigated. On the other hand, several population-based screening studies suggest that spontaneous regression also predominantly occurs in stage 1 and 2 patients

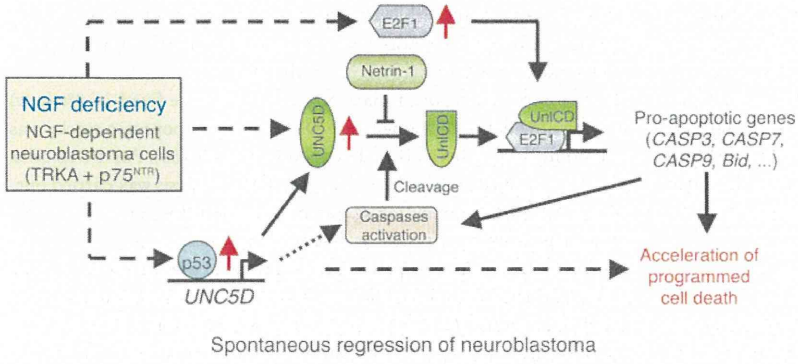

Figure 9
Model of UNC5D-mediated cell death in NGF-dependent NB cells.

who have localized tumors (36–38). It should be noted that induction and nuclear localization of UNC5D were observed in regressing NB tissue obtained from a patient in stage 1, who had been found by mass screening at the age of 6 months (Figure 4F), which suggests that UNC5D is involved in NB regression. Moreover, the number of neuronal cells isolated from the DRG of *Unc5d*$^{-/-}$ mice was significantly higher than that from wild-type mice (Table 1), and *Unc5d*$^{-/-}$ sympathetic neurons showed the attenuated response to NGF removal (Figure 3F). These findings suggest that UNC5D may have a crucial function in the NGF depletion–triggered PCD process occurring in both developing peripheral neurons and sympathoadrenal lineage-derived NBs dependent on NGF for survival. Because our studies have been mainly conducted using in vitro cell systems, our findings give suggestive clues for developmentally regulated PCD in developing sympathetic neurons with NGF dependence. Further approaches using sympathetic neural progenitor cells should facilitate a better understanding of the molecular mechanism of NGF deficiency–induced neuronal PCD.

Here, we found that netrin-1 protein was positive only in some stromal cells following immunohistochemistry (Figure 1B). In regressing NBs, netrin-1 was almost negative (Figure 4F). Therefore, similar to NGF, the amount of netrin-1 in NB tissues appears to be relatively deficient, which supports the role of UNC5D and its proapoptotic function in spontaneously regressing NBs. Recently, it has been reported that netrin-1 may act as a survival factor for enhancing cell growth and invasion in an autocrine manner in metastatic stage 4 NBs compared with stage 4s tumors (39). If so, the aggressive behavior of stage 4 NB may be associated with inhibition of UNC5D proapoptotic function by netrin-1 produced by tumor cells.

Previous reports have suggested that the UNC5 family plays a significant role in cancers. Expression of UNC5A–UNC5C is downregulated in various cancers (40). *UNC5D* is mapped to chromosome 8p12. This region is frequently aberrant in many cancers (41) and may harbor some candidate tumor suppressor genes, such as *SFRP1* (42), *HTPAP* (43), and a breast cancer susceptibility gene (44). *UNC5D* itself is also included in the homozygously deleted region at D8S87 in prostate cancer (45), in the region with some recurrent breaks in breast cancer (46), and in the deleted region in muscle-invasive bladder cancer (47). In addition, the *UNC5D* promoter region is hypermethylated in lung cancer (48), which indicates that UNC5D may be a candidate tumor suppressor for various human cancers. However, in NBs, the frequency of allelic loss at the *UNC5D* locus was only 16%, according to array-CGH analysis of 112 primary NBs (A. Nakagawara, unpublished observations), and promoter hypermethylation was observed at all stages of NB to some extent, without any correlation to prognosis (A. Nakagawara and T. Ushijima, unpublished observations). Nevertheless, *UNC5D* was upregulated by treatment with both histone deacetylase inhibitors and methylation inhibitors in several NB cell lines (data not shown), which indicates that epigenetic modifications may regulate UNC5D expression in NBs. Importantly, UNC5D was induced in response to NGF deprivation and had the ability to induce cell death in NBs under the condition of netrin-1 deficiency, providing support for the notion that dependent receptor UNC5D may function as a conditional tumor suppressor in NBs.

A putative caspase cleavage site exists in the majority of dependence receptors identified so far (13, 23), which suggests that caspase cleavage is an important event in the regulation of the proapoptotic function of dependence receptors. Cleaved UnICD may translocate into the nucleus (49, 50). In fact, the γ-secretase–generated intracellular domain of DCC translocates into the nucleus and has transcriptional activity (51). In the present study, we uncovered the molecular mechanism of dependence receptor UNC5D-mediated apoptosis through caspase cleavage. Notably, the VDVID^{416} site in UNC5D was targeted by not only caspase 3, but also caspase 2, distinct from other UNC5 family members. Caspase 2 plays a critical role in intrinsic and extrinsic apoptotic processes as both initiator and effector (52). More importantly, a caspase 2–dependent pathway is required for neuronal cell death induced by NGF deprivation to complete the highly organized nervous system in the body (53). On the other hand, induction and caspase cleavage of UNC5D were observed in several cell lines in response to various apoptotic stimuli besides NGF withdrawal, which indicates that UNC5D is a common proapoptotic molecule involved in various apoptotic signaling pathways.

We showed here that UNC5D exerted its ability to induce apoptosis through translocation of caspase-cleaved UnICD into the nucleus, where it interacts with the E2F1 transcription factor. Of the E2F family members, induction of apoptosis may be mainly executed by E2F1 (32). In response to apoptotic stimuli, E2F1 itself is stabilized, and the target genes involved in activation or execution of apoptotic program are upregulated (31). However, the mechanism underlying gene-specific regulation by which E2F1 selects proproliferative or proapoptotic target genes has never been fully understood. Recently, Lees and colleagues documented that E2F1 forms a transcriptionally active complex with pRB and P/CAF specially recruited to E2F1 apoptotic target genes in response to genotoxic stress (54). Similarly, our findings revealed that nuclear UnICD only selectively enhanced the transcription of proapoptotic targets of E2F1, without significant changes in the targets promoting proliferation and survival, which suggests that nuclear UnICD may be a component of the E2F1 transcriptional complex that modulates the activity of E2F1 for apoptosis induction.

Important roles of p53 and E2F1 as well as caspase 2 during NGF depletion–induced neuronal cell death have long been implicated (6, 8, 9, 53). Considering that UNC5D is a transcrip-

tional target of the p53 family and responds to various apoptotic stimuli, including NGF withdrawal, our present results suggest that UNC5D is involved in NGF deprivation–induced PCD, which contributes to spontaneous regression of NB, and possibly developmentally regulated cell death of neural crest–derived neurons with NGF dependence. Identifying the more detailed signaling pathways may provide tools to develop novel therapeutic strategies against aggressive NBs, which are independent of NGF for cell growth and metastasis.

Methods

Patients and tumor samples. 108 fresh NB tumor tissues were obtained from patients who had been diagnosed between 1995 and 1999 in Japan. In all, 29 tumors were stage 1, 16 stage 2, 6 stage 4s, 36 stage 3, and 21 stage 4.

Cell culture, transfection, and RNAi. NB cell lines were cultured in RPMI medium. Other cells used in this study were grown in DMEM medium (Sigma-Aldrich) supplemented with 10% (v/v) FBS. Fugene HD (Roche) was used for cell transfections, following the manufacturer's instructions. siRNAs were obtained from Dharmacon.

Preparation of the UNC5D-specific antibody. To generate the UNC5D-specific antibody, rabbit antiserum was raised against the peptides (amino acids 937–956) of human UNC5D and purified with the affinity purification column by MBL Co. Ltd. Specificity of the antibody was confirmed by IB analysis.

Generation of Unc5d$^{-/-}$ mice and isolation of primary sympathetic neurons. The *Unc5d* targeting vector was constructed using a BAC clone isolated from a C57BL/6J mouse genomic library (RPCI-23, 372F8 clone; Invitrogen). The 6.5-kb EcoR V–Sma I fragment spanning upstream of the first exon of *Unc5d* was used as the long arm, and the 1.2-kb Pst I fragment in the first intron as the short arm. The 1.0-kb Sma I–Pst I fragment containing the first exon served as the targeted sequence. The targeted sequence was replaced by the *loxP-PGK-Neo-loxP* selection cassette including *PGK-DTA*. The targeting construct was linearized and electroporated into F1 mouse-derived (129/SvJ × C57BL/6J) ES cells. G418-resistant ES clones were screened by PCR and further verified with Southern blotting using both internal and external probes. Finally, 3 independent germline-transmitting chimeric mice were obtained and used after removing *PGK-Neo* by *cre* cRNA microinjection into the zygote.

Sympathetic neurons were obtained by enzymatic dissociation of SCG from P0 newborn mice. 3×10^3 cells/well were plated in 6-well dishes (Collagen Type IV cellware; BD Biosciences) in MEM supplemented with 10% (v/v) FBS, 2 mM uridine (Sigma-Aldrich), 2 mM fluorodeoxyuridine (Sigma-Aldrich), and 50 ng/ml mouse NGF (Harlan) for 5 days. Continuously, cells were cultured with or without 50 ng/ml NGF for the following 3 days and observed every 12 hours. In the NGF depletion group, 1% volume anti-NGF antiserum (Accurate Chemical & Scientific Corp.) was added to the medium.

Semiquantitative and quantitative RT-PCR analysis. Total RNA was prepared using an RNeasy mini kit (Qiagen) according to the manufacturer's protocol. See Supplemental Methods for details.

Immunofluorescence and immunohistochemistry. Frozen sections of NB clinical samples as well as cultured cells were fixed with 4% (w/v) formaldehyde and then incubated with the corresponding antibodies. Nuclei were stained with DAPI (Vector Laboratories). Cells were visualized under a Fluoview laser scanning confocal microscope (Olympus). NB tissue samples were obtained from the patients in stage 1 who had been found by mass screening at the age of 6 months and had favorable biological characteristics, including age less than 1 year, single copy of *MYCN*, and favorable histology. Histology of the tissues was shown by H&E staining.

Immunohistochemical analysis was carried out using paraffin-embedded tissues as described previously (55).

Apoptosis assay. Cell death was analyzed using the Trypan blue staining procedure (14). Apoptosis was monitored using an in situ cell death detection Kit (Roche). Nuclei were stained with DAPI.

For apoptosis assay of primary NB cells, cells were fixed in 4% (w/v) paraformaldehyde and stained with DAPI. Percent apoptotic nuclei was counted in 3 separate fields as described previously (56). For PC12 cells, cells were collected at each time point, and FACS analysis was carried out.

Colony formation assay and soft-agar assay. The colony formation assay and soft-agar assay were performed as described previously (57).

IP and IB. IP and IB were performed as described previously (57), using nuclear extracts or whole cell lysates. Whole cell lysates were prepared as described previously (25). See Supplemental Methods for details.

In vitro caspase cleavage assay. See Supplemental Methods and ref. 58.

Luciferase reporter assay. The luciferase reporter assay was conducted using a Dual-Luciferase Reporter Assay System (Promega) as described previously (57). pM-VP16 expression vector was used as a positive control.

Treatment of primary NB cells and PC12 cells with NGF. Primary NB cells were dissected from fresh NB tissues at 4°C, seeded at a density of $1–2 \times 10^5$ cells/well in a 6-well plate, and cultured in RPMI/OPI medium (Nissui Pharmaceutical) supplemented with 10% (v/v) FBS and antibiotics. PC12 cells were seeded at a density of 1×10^6 cells per 10-cm dish in DMEM medium supplemented with 5% (v/v) FBS and 10% (v/v) horse serum. NGF was added on the next day at a final concentration of 50 ng/ml. Primary cells were grown for 4 days, and PC12 cells for 6 days, with a change of medium containing NGF every 2–3 days. In the NGF withdrawal group, anti-NGF antibody was added at a final concentration of 0.1 μg/ml. The adherent primary NB cells were subjected to subsequent studies.

For knockdown experiments, PC12 cells were seeded at a density of 2×10^5 cells/well in collagen-coated 6-well plates. Accell siRNA against rat UNC5D (Dharmacon) was transduced into PC12 cells twice for long-term knockdown according to the manufacturer's protocol. Control Accell siRNA was used as a negative control. Cells were then subjected to NGF treatment.

Statistics. Statistical analysis was performed using Stata 6.0 software (Stata Corp.). 2-tailed Student's *t* test was used to explore possible associations between UNC5D expression and other factors. The distinction between high and low levels of *UNC5D* mRNA was based on the median value of the real-time PCR data (median value, 1.47; $P = 0.0032$), regardless of tumor stage, *MYCN* copy number, or survival. Kaplan-Meier survival curves were drawn, and survival distributions were compared using the log-rank test. Cox regression models were used to explore associations among UNC5D, age, *MYCN* copy number, TRKA, origin, and survival. A *P* value less than 0.05 was considered significant.

Study approval. Studies using clinical NB samples were approved by the Institutional Review Board of Chiba Cancer Center. Written informed consent was provided by the patients' parents. The Review Board for Animal Life Science of Chiba Cancer Center approved all animal experiments.

Acknowledgments

We thank Kohei Akazawa for statistical analysis, Hiroki Nagase for helpful discussion, and Takahiro Inoue for the *Unc5d*$^{-/-}$ mouse. This work was funded in part by a Grant-in-Aid from the Ministry of Health, Labor, and Welfare of Japan for the Third Term Comprehensive Control Research for Cancer; by a grant from Takeda Science Foundation; by the National Cancer Center Research and Development Fund; and by Grants-in-Aid for Scientific Research from the Ministry of Education, Culture, Sports, Science and Technology of Japan (JSPS KAKENHI grants 19591271, 24249061, 21591378, and 24591566).

Received for publication July 25, 2012, and accepted in revised form April 25, 2013.

Address correspondence to: Akira Nakagawara, Division of Biochemistry and Innovative Cancer Therapeutics and Children's Cancer Research Center, Chiba Cancer Center Research Institute, 666-1 Nitona-Chou, Chuo-Ku, Chiba-city, Chiba 260-8717, Japan. Phone: 81.43.264.5431; Fax: 81.43.265.4459; E-mail: akiranak@chiba-cc.jp.

Seiki Haraguchi's present address is: Animal Breeding and Reproduction Division, National Agriculture and Food Research Organization, Tsukuba, Japan.

1. D'Angio GJ, Evans AE, Koop CE. Special pattern of widespread neuroblastoma with a favourable prognosis. *Lancet.* 1971;1(7708):1046–1049.
2. Nakagawara A, et al. Association between high levels of expression of the TRK gene and favorable outcome in human neuroblastoma. *N Engl J Med.* 1993; 328(12):847–854.
3. Christiansen H, et al. Neuroblastoma: inverse relationship between expression of N-myc and NGF-r. *Oncogene.* 1990;5(3):437–440.
4. Nakagawara A, Azar CG, Scavarda NJ, Brodeur GM. Expression and function of TRK-B and BDNF in human neuroblastomas. *Mol Cell Biol.* 1994; 14(1):759–767.
5. Nakagawara A. The NGF story and neuroblastoma. *Med Pediatr Oncol.* 1998;31(2):113–115.
6. Aloyz RS, et al. p53 is essential for developmental neuron death as regulated by the TrkA and p75 neurotrophin receptors. *J Cell Biol.* 1998; 143(6):1691–1703.
7. Jacobs WB, et al. p63 is an essential proapoptotic protein during neural development. *Neuron.* 2005; 48(5):743–756.
8. Persengiev SP, Kondova II, Kilpatrick DL. E2F4 actively promotes the initiation and maintenance of nerve growth factor-induced cell differentiation. *Mol Cell Biol.* 1999;19(9):6048–6056.
9. O'Hare MJ, et al. Induction and modulation of cerebellar granule neuron death by E2F-1. *J Biol Chem.* 2000;275(33):25358–25364.
10. Lee S, et al. Neuronal apoptosis linked to EglN3 prolyl hydroxylase and familial pheochromocytoma genes: developmental culling and cancer. *Cancer Cell.* 2005;8(2):155–167.
11. Schlisio S, et al. The kinesin KIF1Bbeta acts downstream from EglN3 to induce apoptosis and is a potential 1p36 tumor suppressor. *Genes Dev.* 2008; 22(7):884–893.
12. Munirajan AK, et al. KIF1Bbeta functions as a haploinsufficient tumor suppressor gene mapped to chromosome 1p36.2 by inducing apoptotic cell death. *J Biol Chem.* 2008;283(36):24426–24434.
13. Bredesen DE, Mehlen P, Rabizadeh S. Receptors that mediate cellular dependence. *Cell Death Differ.* 2005;12(8):1031–1043.
14. Mehlen P, et al. The DCC gene product induces apoptosis by a mechanism requiring receptor proteolysis. *Nature.* 1998;395(6704):801–804.
15. Bordeaux MC, et al. The RET proto-oncogene induces apoptosis: a novel mechanism for Hirschsprung disease. *EMBO J.* 2000;19(15):4056–4063.
16. Llambi F, Causeret F, Bloch-Gallego E, Mehlen P. Netrin-1 acts as a survival factor via its receptors UNC5H and DCC. *EMBO J.* 2001;20(11):2715–2722.
17. Wang H, et al. A newly identified dependence receptor UNC5H4 is induced during DNA damage-mediated apoptosis and transcriptional target of tumor suppressor p53. *Biochem Biophys Res Commun.* 2008;370(4):594–598.
18. Thibert C, et al. Inhibition of neuroepithelial patched-induced apoptosis by sonic hedgehog. *Science.* 2003;301(5634):843–846.
19. Matsunaga E, et al. RGM and its receptor neogenin regulate neuronal survival. *Nat Cell Biol.* 2004; 6(8):749–755.
20. Mourali J, et al. Anaplastic lymphoma kinase is a dependence receptor whose proapoptotic functions are activated by caspase cleavage. *Mol Cell Biol.* 2006;26(16):6209–6222.
21. Stupack DG, et al. Apoptosis of adherent cells by recruitment of caspase-8 to unligated integrins. *J Cell Biol.* 2001;155(3):459–470.
22. Ohira M, et al. Expression profiling and characterization of 4200 genes cloned from primary neuroblastomas: identification of 305 genes differentially expressed between favorable and unfavorable subsets. *Oncogene.* 2003;22(35):5525–5536.
23. Mehlen P, Mazelin L. The dependence receptors DCC and UNC5H as a link between neuronal guidance and survival. *Biol Cell.* 2003;95(7):425–436.
24. Tanikawa C, Matsuda K, Fukuda S, Nakamura Y, Arakawa H. p53RDL1 regulates p53-dependent apoptosis. *Nat Cell Biol.* 2003;5(3):216–223.
25. Williams ME, et al. UNC5A promotes neuronal apoptosis during spinal cord development independent of netrin-1. *Nat Neurosci.* 2006;9(8):996–998.
26. Lu X, et al. The netrin receptor UNC5B mediates guidance events controlling morphogenesis of the vascular system. *Nature.* 2004;432(7014):179–186.
27. Przyborski SA, Knowles BB, Ackerman SL. Embryonic phenotype of Unc5h3 mutant mice suggests chemorepulsion during the formation of the rostral cerebellar boundary. *Development.* 1998; 125(1):41–50.
28. Deckwerth TL, et al. BAX is required for neuronal death after trophic factor deprivation and during development. *Neuron.* 1996;17(3):401–411.
29. Schroeter EH, Kisslinger JA, Kopan R. Notch-1 signalling requires ligand-induced proteolytic release of intracellular domain. *Nature.* 1998; 393(6683):382–386.
30. Kimberly WT, Zheng JB, Guenette SY, Selkoe DJ. The intracellular domain of the beta-amyloid precursor protein is stabilized by Fe65 and translocates to the nucleus in a notch-like manner. *J Biol Chem.* 2001;276(43):40288–40292.
31. Pediconi N, et al. Differential regulation of E2F1 apoptotic target genes in response to DNA damage. *Nat Cell Biol.* 2003;5(6):552–558.
32. Iaquinta PJ, Lees JA. Life and death decisions by the E2F transcription factors. *Curr Opin Cell Biol.* 2007; 19(6):649–657.
33. Johnson DG, Ohtani K, Nevins JR. Autoregulatory control of E2F1 expression in response to positive and negative regulators of cell cycle progression. *Genes Dev.* 1994;8(13):1514–1525.
34. Williams ME, Strickland P, Watanabe K, Hinck L. UNC5H1 induces apoptosis via its juxtamembrane region through an interaction with NRAGE. *J Biol Chem.* 2003;278(19):17483–17490.
35. Llambi F, et al. The dependence receptor UNC5H2 mediates apoptosis through DAP-kinase. *EMBO J.* 2005;24(6):1192–1201.
36. Sawada T, Hirayama M, Nakata T, Takeda T, Takasugi N, Mori T, Maeda K, Koide R, Hanawa Y, Tsunoda A, et al. Mass screening for neuroblastoma in infants in Japan. Interim report of a mass screening study group. *Lancet.* 1984;2(8397):271–273.
37. Woods WG, et al. A population-based study of the usefulness of screening for neuroblastoma. *Lancet.* 1996;348(9043):1682–1687.
38. Schilling FH, et al. Children may not benefit from neuroblastoma screening at 1 year of age. Updated results of the population based controlled trial in Germany. *Cancer Lett.* 2003;197(1–2):19–28.
39. Delloye-Bourgeois C, et al. Netrin-1 acts as a survival factor for aggressive neuroblastoma. *J Exp Med.* 2009;206(4):833–847.
40. Thiebault K, et al. The netrin-1 receptors UNC5H are putative tumor suppressors controlling cell death commitment. *Proc Natl Acad Sci U S A.* 2003; 100(7):4173–4178.
41. Payne SR, Kemp CJ. Tumor suppressor genetics. *Carcinogenesis.* 2005;26(12):2031–2045.
42. Huang J, et al. Down-regulation of SFRP1 as a putative tumor suppressor gene can contribute to human hepatocellular carcinoma. *BMC Cancer.* 2007;7:126.
43. Wu X, et al. HTPAP gene on chromosome 8p is a candidate metastasis suppressor for human hepatocellular carcinoma. *Oncogene.* 2006;25(12):1832–1840.
44. Seitz S, et al. Strong indication for a breast cancer susceptibility gene on chromosome 8p12-p22: linkage analysis in German breast cancer families. *Oncogene.* 1997;14(6):741–743.
45. Prasad MA, Trybus TM, Wojno KJ, Macoska JA. Homozygous and frequent deletion of proximal 8p sequences in human prostate cancers: identification of a potential tumor suppressor gene site. *Genes Chromosomes Cancer.* 1998;23(3):255–262.
46. Véronique GB, et al. Comprehensive profiling of 8p11-12 amplification in breast cancer. *Mol Cancer Res.* 2005;3(12):655–667.
47. Koed K, et al. High-density single nucleotide polymorphism array defines novel stage and location-dependent allelic imbalances in human bladder tumors. *Cancer Res.* 2005;65(1):34–45.
48. Rauch TA, et al. High-resolution mapping of DNA hypermethylation and hypomethylation in lung cancer. *Proc Natl Acad Sci U S A.* 2008;105(1):252–257.
49. Wells A, Marti U. Signalling shortcuts: cell-surface receptors in the nucleus? *Nat Rev Mol Cell Biol.* 2002; 3(9):697–702.
50. Johnson HM, Subramaniam PS, Olsnes S, Jans DA. Trafficking and signaling pathways of nuclear localizing protein ligands and their receptors. *Bioessays.* 2004;26(9):993–1004.
51. Taniguchi Y, Kim SH, Sisodia SS. Presenilin-dependent "gamma-secretase" processing of deleted in colorectal cancer (DCC). *J Biol Chem.* 2003; 278(33):30425–30428.
52. Troy CM, Shelanski ML. Caspase-2 redux. *Cell Death Differ.* 2003;10(1):101–107.
53. Troy CM, et al. Death in the balance: alternative participation of the caspase-2 and -9 pathways in neuronal death induced by nerve growth factor deprivation. *J Neurosci.* 2001;21(14):5007–5016.
54. Ianari A, et al. Proapoptotic function of the retinoblastoma tumor suppressor protein. *Cancer Cell.* 2009;15(3):184–194.
55. Ando K, et al. Expression of TSLC1, a candidate tumor suppressor gene mapped to chromosome 11q23, is downregulated in unfavorable neuroblastoma without promoter hypermethylation. *Int J Cancer.* 2008;123(9):2087–2094.
56. Stefanis L, Park DS, Friedman WJ, Greene LA. Caspase-dependent and -independent death of camptothecin-treated embryonic cortical neurons. *J Neurosci.* 1999;19(15):6235–6247.
57. Li Y, et al. A novel HECT-type E3 ubiquitin protein ligase NEDL1 enhances the p53-mediated apoptotic cell death in its catalytic activity-independent manner. *Oncogene.* 2008;27(26):3700–3709.
58. Foveau B, et al. Amplification of apoptosis through sequential caspase cleavage of the MET tyrosine kinase receptor. *Cell Death Differ.* 2007;14(4):752–764.